OPEN

Mucin 1 Regulates *Cox-2* Gene in Pancreatic Cancer

Sritama Nath, PhD, Lopamudra Das Roy, PhD,* Priyanka Grover, BSc,* Shanti Rao, BSc,† and Pinku Mukherjee, PhD**

Objective: Eighty percent of pancreatic ductal adenocarcinomas (PDAs) overexpress mucin 1 (MUC1), a transmembrane mucin glycoprotein. MUC1^{high} PDA patients also express high levels of cyclooxygenase 2 (COX-2) and show poor prognosis. The cytoplasmic tail of MUC1 (MUC1-CT) partakes in oncogenic signaling, resulting in accelerated cancer progression. Our aim was to understand the regulation of Cox-2 expression by MUC1.

Methods: Levels of COX-2 and MUC1 were determined in MUC1$^{-/-}$, MUC1^{low}, and MUC1^{high} PDA cells and tumors using reverse transcriptase–polymerase chain reaction, Western blot, and immunohistochemistry. Proliferative and invasive potential was assessed using MTT and Boyden chamber assays. Chromatin immunoprecipitation was performed to evaluate binding of MUC1-CT to the promoter of *COX-2* gene.

Results: Significantly higher levels of COX-2 mRNA and protein were detected in MUC1^{high} versus MUC1$^{low/null}$ cells, which were recapitulated in vivo. In addition, deletion of MUC1 gene and transient knockdown of MUC1 led to decreased COX-2 level. Also, MUC1-CT associated with the *COX-2* promoter at ~1000 base pairs upstream of the transcription start site, the same gene locus where nuclear factor κB p65 associates with the *COX-2* promoter.

Conclusions: Data supports a novel regulation of *COX-2* gene by MUC1 in PDA, the intervention of which may lead to a better therapeutic targeting in PDA patients.

Key Words: pancreatic cancer, mucin 1 cytoplasmic tail, cyclooxygenase 2, NF-κB p65

Abbreviations: MUC1, mucin 1, MUC1-CT, MUC1 cytoplasmic tail, PDA, pancreatic ductal adenocarcinoma, PC, pancreatic cancer, Cox-2, cyclooxygenase 2, PGE_2, prostaglandin E_2, UTR, untranslated region, CRE, cAMP response element, IHC, immunohistochemistry

(*Pancreas* 2015;44: 909–917)

Pancreatic ductal adenocarcinoma is a lethal disease and is the fourth leading cause of cancer-related deaths in the United States. Because of the absence of effective screening methods, efforts have been focused on developing new treatment modalities. However, most new clinical trials have shown limited survival benefit for the patients. Chronic inflammation is now considered as 1 of the 7 hallmarks of cancer. Cyclooxygenase 2 (Cox-2) is an inducible proinflammatory enzyme that converts arachidonic acid to prostaglandins. In cancer, the major functional metabolite of Cox-2 is prostaglandin E_2 (PGE_2). Cyclooxygenase 2 and PGE_2 are frequently overexpressed in a vast majority of epithelial malignancies,[1,2] including pancreatic ductal adenocarcinoma (PDA) (>60%),[3] and is known to be associated with enhanced inflammation, metastasis, and immune suppression within the tumor microenvironment.[4–7] Cyclooxygenase 2 inhibition has been successfully used as a chemopreventive agent against colon polyps.[8] However, even in combination with chemotherapeutic agents, Cox-2 inhibition has not been useful in patients with PDA.[9] This is possibly because regulation of Cox-2 is not well understood in PDA. Mucin 1 (MUC1), a heavily glycosylated membrane tethered glycoprotein normally expressed on glandular epithelial cells, becomes aberrantly hypoglycosylated and vastly overexpressed in malignant cells.[10] The cytoplasmic tail of the tumor-induced form of MUC1 (MUC1-CT) associates with several oncogenic proteins including β-catenin and nuclear factor κB (NF-κB).[11] The complex then translocates to the nucleus and promotes transcription of tumor-promoting genes.[12,13] Approximately 80% of human PDA overexpresses the tumor form of MUC1 (tMUC1)[10] and is correlated with poor prognosis. We therefore sought to assess if tMUC1 may be involved in the regulation of Cox-2 in PDA. We have recently generated a mouse model of spontaneous PDA that expresses human MUC1 (PDA.MUC1 mice).[14,15] PDA.MUC1 mice develop a spectrum of premalignant lesions called pancreatic intraepithelial neoplasias that progress to adenocarcinoma with 100% penetrance. In most instances, the tumors have a moderately differentiated ductal morphology with extensive stromal desmoplasia commonly observed in humans. Similar to human disease, these mice develop metastases primarily in the liver, peritoneum, and lungs. Along with overexpression of tMUC1, the tumors exhibit high levels of Cox-2 and PGE_2.[14] PDA.MUC1 mice are highly resistant to gemcitabine and celecoxib (a specific Cox-2 inhibitor) when each drug is administered separately. However, when treated with a combination of MUC1 vaccine, celecoxib, and gemcitabine, the antitumor response is clinically significant.[15] In addition, the PDA.MUC1 cells generated from these tumors exhibit increased multidrug resistance genes.[13,15] Thus, it becomes imperative to understand the regulation of Cox-2 overexpression in PDA and design alternative therapeutics to block Cox-2 activation.

We demonstrate a novel regulation of *Cox-2* gene expression by MUC1, suggesting MUC1 as an alternative target to prevent Cox-2 overexpression and associated aggressiveness in PDA.

MATERIALS AND METHODS

Mouse Model and Cell Lines

PDA.Muc1KO and PDA.MUC1 as described by Besmer et al[16] are used. KCM and KCKO cell lines were generated from PDA.MUC1 and PDA.Muc1 KO mice, respectively.[16]

Human PDA cell lines Hs766T, Capan-2, HPAFII, HPAC and CFPAC, BxPC3, Capan-1, and MIA-PaCa-2 were obtained from ATCC (Manassas, Va). BXPC3 cells were stably transfected with

From the *Department of Biology, University of North Carolina at Charlotte, Charlotte; and †School of Medicine, University of North Carolina at Chapel Hill, Chapel Hill, NC.

Received for publication October 1, 2014; accepted March 25, 2015.

Reprints: Pinku Mukherjee, PhD, Department of Biological Sciences, University of North Carolina–Charlotte, 9201 University City Blvd, Charlotte, NC 28223 (e-mail: pmukherj@uncc.edu).

This study was supported by the National Institutes of Health (RO1 CA118944-01A1) and Irwin Belk Endowment Funds.

The authors declare no conflict of interest.

Supplemental digital contents are available for this article. Direct URL citations appear in the printed text and are provided in the HTML and PDF versions of this article on the journal's Web site (www.pancreasjournal.com).

empty vector or vector containing full-length *MUC1* to generate BxPC3.Neo and BxPC3.MUC1 cells, respectively. Dr Michael Hollingsworth generously donated mouse Panc02.Neo and Panc02.MUC1 cell lines.

Transient Knockdown of Target Genes Using siRNA

Cells were plated in a 6-well plate in antibiotic-free complete media and upon reaching 30% confluence and were transfected with 100 to 200 nM of smart pool MUC1 siRNA (DHARMACON; Thermo Fisher Scientific, Waltham, Mass), 200 nM of NF-κB siRNA (Santa Cruz Biotechnology, Santa Cruz, Calif), or 100 to 200 nM of scramble control siRNA (Cell Signaling Technology, Danvers, Mass) using Lipofectamine 2000 (Invitrogen, Grand Island, NY) for 5 to 6 hours in serum-free Opti-MEM media (Invitrogen). Whole cell lysates prepared at 48, 72, and 96 hours post siRNA treatment were subjected to Western blotting to determine the efficiency of the knockdown.

Western Blots

Cell lysates were prepared using RIPA buffer, and 30 to 60 μg of protein was subjected to denaturing sodium dodecyl sulfate–polyacrylamide gel electrophoresis (SDS-PAGE) and Western blot. The polyvinylidene fluoride membrane was probed with anti-MUC1 antibody CT2, anti–NF-κB p65 (Cell Signaling Technology), anti-Cox-2, anti–lamin A/C, and anti–β-actin (Santa Cruz Biotechnology) antibodies. Appropriate secondary antibodies conjugated to horseradish peroxidase were used, and protein detected using the chemiluminescence kit. All antibodies were used according to manufacturer's recommendations.

Preparation of Nuclear Extract

Cells were grown in 10-cm plate and upon reaching 85% confluence were lysed using the EMD Millipore nuclear extraction kit to isolate the nuclear and the cytosolic fractions.

Serum PGE_2 Metabolite by Enzyme-Linked Immunosorbent Assay

Serum PGE_2 levels were determined using a specific enzyme-linked immunosorbent assay (ELISA) kit (Cayman Pharmaceuticals, Ann Arbor, Mich) that measures for the prostaglandin E_2 metabolite (PGEM) (13,14-dihydro 15-keto prostaglandin A_2). The protocol was followed as recommended by the manufacturer. Results were expressed in picograms per milliliter of PGE_2 or PGEM.

Human PDA Samples

Tissue sections of human pancreatic adenocarcinoma (PDA) and normal pancreas were obtained from the National Institutes of Health/National Cancer Institute tissue repository (http://seer.cancer.gov/biospecimen). The sera of patients with pancreatic cancer (PC) from different stages were also obtained from the National Cancer Institute.

Mouse PDA Samples

Two-month-old nude mice were injected with 5×10^6 BxPC3Neo or BxPC3.MUC1 cells in the flank region, and the tumors were allowed to grow for 2 months. Tumors were harvested for immunohistochemistry (IHC) and tumor lysate. PDA.MUC1 and PDA.MUC1 knockout mice between 16 and 40 weeks of age were killed, and tumors were harvested. Paraffin-embedded blocks of formalin-fixed tumor sections were made by the Histology Core at Carolinas Medical Center. Four-micron-thick sections were prepared for IHC staining.

Immunohistochemistry

Standard IHC method was followed. Primary antibodies used were as follows: Armenian hamster anti–MUC1-CT antibody CT2 (1:50, gift from Dr Gendler) and goat anti–COX-2 (1:100; Santa Cruz Biotechnology). Secondary antibodies used were anti–hamster (1:250; Jackson Laboratory, Bar Harbor, Maine) and anti–goat (1:100; Dako, Carpenteria, Calif) IgGs conjugated to horseradish peroxidase. Immunopositivity was assessed using light microscopy, and images were taken at 200× magnification.

Chromatin Immunoprecipitation

Cells grown to near 80% confluence were cross-linked with formaldehyde (Sigma) at room temperature for 10 minutes. Cross-linked chromatin prepared with a commercial chromatin immunoprecipitation (ChIP) assay kit (EZ-Magna ChIP; Millipore) was immunoprecipitated with normal Armenian hamster IgG (1:20) (Santa Cruz Biotechnology), anti–MUC1-CT antibody (CT2) (1:15), and anti–NF-κB p65 (1:20) antibody. IgG was used as a negative control for the immunoprecipitation step. Input DNA (2%) and DNA isolated from the precipitated chromatin were amplified by polymerase chain reaction (PCR) using mouse- or human-specific primers flanking the promoter region containing the NF-κB–binding site (ChIP region I) or distant sites from the promoter region (ChIP region II). Chromatin immunoprecipitation region II was used as a negative control to evaluate specificity of association between MUC1-CT and NF-κB p65 to the promoter region of *Ptgs2/PTGS2* gene. Sequence of the primers is available upon request.

Semiquantitative and Quantitative Reverse Transcriptase–PCR

TRIzol (Invitrogen) was used to extract total RNA according to the manufacturer's protocol; 1 to 2 μg of the extracted RNA was used as template for semiquantitative reverse transcriptase (RT)–PCR reaction (Access quick RT-PCR kit; Promega, Madison, Wis) and real-time RT-PCR (KAPA SYBR Fast One-step qRT-PCR kit, Willmington, Mass). Sequence of the primers is available upon request.

Cell Growth by MTT Assay

Ten thousand cells plated in a 96-well plate were permitted to grow overnight. Cells were left untreated or treated with celecoxib (Pfizer, China) for 24 hours. Next, MTT (Biotium, Hayward, Calif) solution was added (10 μL/well) to cells incubated for an additional 3 to 4 hours. In the final step, media was removed, formazan was dissolved in dimethyl sulfoxide (200 μL/well), and the absorbance read using an ELISA plate reader.

Invasion Assay

Cells were grown in culture dishes and serum starved for 18 hours before plating for the invasion assay. In a 24-well plate, 50,000 cells in serum-free media with or without celecoxib were plated over Transwell inserts (BD Biosciences, San Jose, California) precoated with reduced growth factor Matrigel (BD Biosciences). Cells were allowed to invade through the matrix toward the serum-supplemented media contained in the bottom chamber over a period of 36 hours. Percent invasion was calculated as follows: (absorbance of samples / absorbance of controls) × 100.

Confocal Microscope

Cells grown on chamber slides were fixed with formalin, permeabilized with 0.5% Tween, and incubated with CT2 conjugated with fluorescein isothiocyanate (Jackson Laboratory) and

anti–NF-κB p65 (rabbit IgG) antibody (Santa Cruz Biotechnology) overnight. On the next day, the cells probed with anti–rabbit IgG antibody conjugated with Alexa fluor (Invitrogen) for 1 hour at room temperature and mounted with ProLong Gold antifade reagent with DAPI. Photographs were taken at 400× using the confocal microscope (Carl Zeiss International, Thornwood, NY).

Densitometric Analyses

The bands on Western blot and semiquantitative RT-PCR were quantified using image analysis software (Image J) from the National Institutes of Health (Bethesda, Md).

Statistical Analysis

Statistical analysis was performed with GraphPad software (La Jolla, Calif). Statistical significance was determined using 1-way analysis of variance (ANOVA), 2-way ANOVA, and *t* test.

RESULTS

Human Primary PDA Expresses High Levels of MUC1 and Cox-2 Protein

Human PDA sections (n = 4 patient tumors) showed high expression of both MUC1 and Cox-2 protein in comparison to the normal pancreas, as indicated by intense brown staining in PDA compared with the normal counterpart (Fig. 1A). In serum of patients with stages 2, 3, and 4 PDA, the PGEM levels increased from a normal level of 63.8 pg/mL (designated as stage 0) to 118 pg/mL in stage 2, 148.8 pg/mL in stage 3, and 210 pg/mL in stage 4 (Fig. 1B), suggesting a stage-dependent increase. There was a 4-fold increase in serum PGEM level of patients with stage 4 versus stage 0. Prostaglandin E_2 metabolite is a measure of Cox-2 enzymatic activity. The same serum samples analyzed for circulating MUC1 showed a similar stage-dependent increase in shed MUC1 level.[17] The data indicated a positive correlation between MUC1 and Cox-2 expression and function in human PDA.

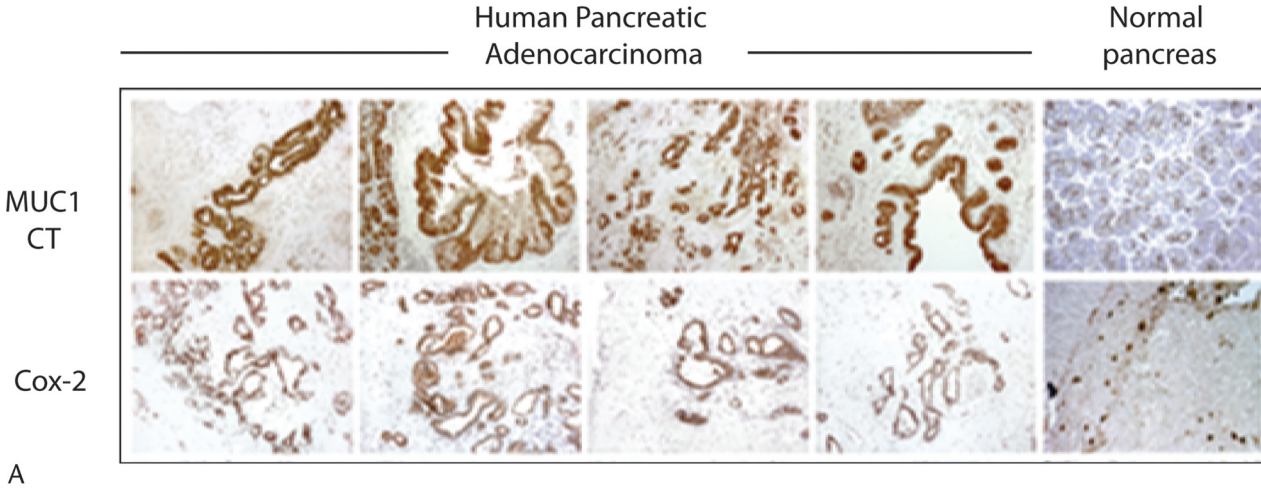

A

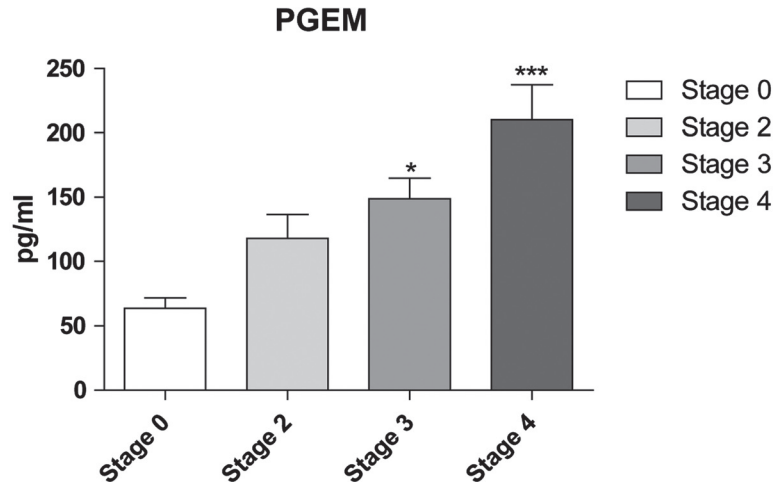

B

FIGURE 1. Expression of MUC1 and COX-2 in human PDA sections and levels of PGEM in the patient serum. A, Immunohistochemistry was performed to compare MUC1 and Cox-2 expression between the human PDA and adjacent normal pancreas tissue sections. Morphologically normal pancreas section shows low apical membranous MUC1 staining and lack of Cox-2 expression. Pancreatic ductal adenocarcinoma samples show strong membranous and cytoplasmic MUC1 staining and show abundant Cox-2 in tumor cells. B, Serum PGE_2 levels from patients with PDA were assessed by PGEM ELISA kit. An average of n = 5 patient samples are shown. One-way ANOVA was performed to determine the statistical significance between the samples (*P = 0.05, ***P = 0.0005).

Positive Correlation Between MUC1 and Cox-2 Expression in Human PDA Cell Lines

A panel of human PDA cell lines expressing various levels of endogenous MUC1 was analyzed for basal MUC1 and Cox-2 protein levels by Western blot. HPAFII, HPAC, CFPAC, and Capan-1 PDA cells expressing high levels of endogenous MUC1 also expressed high Cox-2, whereas Hs766T, Capan-2, and MIA PaCa-2–expressing low levels of endogenous MUC1 expressed low Cox-2 (Fig. 2A). However, this was not the case with BxPC3 cell line that has low endogenous MUC1 but expresses high levels of Cox-2. This may be because BxPC3 cells have normal Kras protooncogene, whereas all other cell lines tested have mutated Kras.[18] Nevertheless, when we overexpressed full-length MUC1 in BxPC3 cells, we did observe a significant increase in Cox-2 levels but no increase in Cox-2 message (Supplemental Figure 1, http://links.lww.com/MPA/A375 and Supplemental Table 1, http://links.lww.com/MPA/A376). Overall, the data validate the existence of a positive correlation between MUC1 and Cox-2 expression in Kras-driven PDA.

Overexpression of MUC1 Augments Cox-2 Expression and a Simultaneous Attenuation Upon MUC1 Down-regulation

Next, we manipulated the levels of MUC1 protein in PDA cells to determine the importance of MUC1 in the regulation of Cox-2 expression. Overexpression of MUC1 in normally low MUC1-expressing Panc02 cells (Panc02.MUC1) caused a 2.6-fold increase in Cox-2 protein level compared with its control counterpart (Panc02.Neo) (Fig. 2B, Supplemental Table 1, http://links.lww.com/MPA/A376, tabulating the densitometric analysis of the blots). Similarly, KCM (MUC1-hi) cells expressed 3.9-fold higher Cox-2 than KCKO (Muc1-null) cells (Fig. 2B,

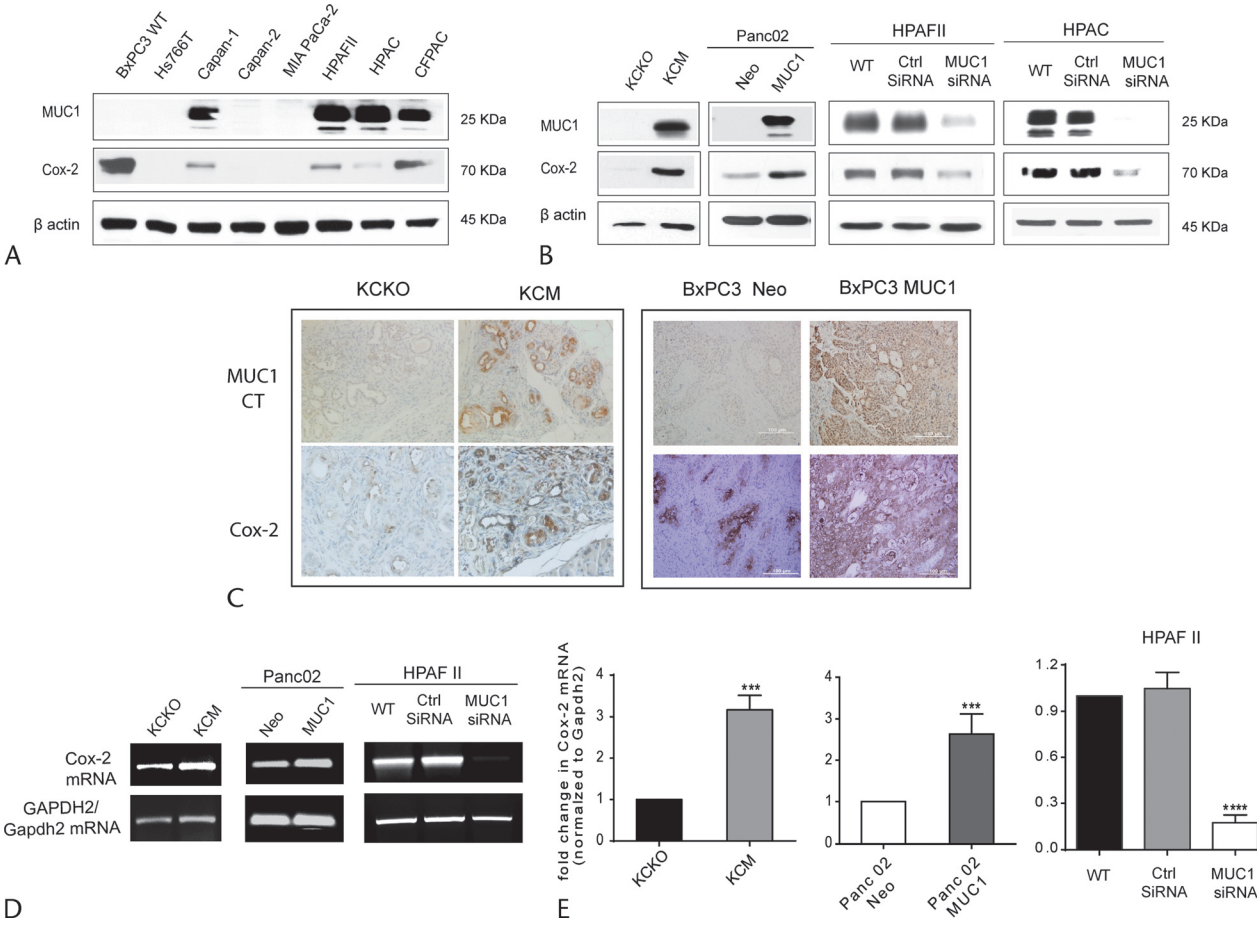

FIGURE 2. Positive correlation between MUC1 and Cox-2 expression in human PC cell lines (in vitro) and in mouse PDA sections. A, Endogenous levels of MUC1 and Cox-2 protein in a panel of human PDA cell lines were evaluated by Western blot using MUC1-CT–specific antibody CT2 and anti–Cox-2 antibody, respectively. Sixty micrograms of protein was loaded for SDS-PAGE. β-Actin was used as loading control. B, Levels of endogenous MUC1 and Cox-2 protein in mouse PDA cell lines, KCM and KCKO, as well as Panc02 cells that were stably infected to overexpress human MUC1. In addition, MUC1 was knockdown in HPAFII and HPAC human PDA cells using a smart pool of MUC1-specific siRNA. Seventy-two hours later, Cox-2 and MUC1 levels were analyzed by Western blot; 60 μg of protein was loaded for SDS-PAGE. C, Immunohistochemistry was performed to compare levels of MUC1 and Cox-2 expression between spontaneously occurring KCKO and KCM tumors at 24 weeks of age. BxPC3 Neo and BxPC3 MUC1 xenografted tumors were stained for MUC1 and Cox-2 expression. KCM and BxPC3.MUC1 tumors showed high levels of Cox-2 in comparison to MUC1-low KCKO and BxPC3 Neo tumors. D, Total mRNA from PDA cell lines were isolated using TRIzol, and the basal levels of Cox-2 mRNA were determined using semiquantitative 1-step RT-PCR kit. E, Graphical representation of fold increase in levels of Cox-2 mRNA normalized to Gapdh2 using real-time quantitative RT-PCR. Unpaired *t* test was performed to determine the statistical significance between KCKO and KCM, n = 3 (***$P < 0.0004$). Unpaired *t* test was performed to determine the statistical significance between Panc02Neo and Panc02MUC1, n = 3 (***$P < 0.001$). One-way ANOVA was performed to determine the statistical significance between HPAFII WT, control siRNA, and MUC1 siRNA-treated samples, n = 3 (****$P < 0.0001$).

Supplemental Table 1, http://links.lww.com/MPA/A376). Upon transient knockdown of MUC1, we observed a 3.5- and 5.8-fold decrease in Cox-2 expression in HPAFII and HPAC cells, respectively (Fig. 2B, Supplemental Table 1, http://links.lww.com/MPA/A376). Thus, manipulation of the MUC1 level altered Cox-2 expression in PDA cells, indicating that *Cox-2* (*Ptgs2/PTGS2*) may be regulated by MUC1.

This was further confirmed in vivo in the PDA.MUC1 and PDA.Muc1KO tumors. Immunohistochemistry was performed to evaluate the coexpression of MUC1 and Cox-2 in situ. PDA.MUC1 tumors expressed higher levels of Cox-2 in comparison to the PDA.Muc1KO tumors, as indicated by the strong brown staining (Fig. 2C, left panel). A similar trend in MUC1 and Cox-2 expression was observed in xenografted human BxPC3.MUC1 and BxPC3.Neo tumors in nude mice. As was expected, BxPC3.MUC1 tumors showed higher Cox-2 expression than MUC1-low BxPC3.Neo tumors (Fig. 2C, right panel).

MUC1 High PDA Cells Express High Levels of Cox-2 mRNA

The level of Cox-2 mRNA in PDA cells expressing variable levels of MUC1 was analyzed by semiquantitative and quantitative RT-PCR. Significant increase and decrease in the Cox-2 transcript level were detected upon MUC1 overexpression or down-regulation, respectively (Fig. 2D, Supplemental Table 2, http://links.lww.com/MPA/A376) by semiquantitative RT-PCR. Furthermore, data obtained using quantitative RT-PCR revealed that the steady-state level of Cox-2 mRNA was 2.4- and 3-fold higher in MUC1-positive Panc02 MUC1 and KCM cells, respectively, compared with Panc02.Neo and KCKO cells (Fig. 2E). Conversely, a 3-fold decrease in Cox-2 mRNA level was observed upon transient knockdown of MUC1 in HPAFII cells (Fig. 2E), indicating that the *Cox-2* gene may be regulated by MUC1 in PDA cells.

MUC1 and NF-κB colocalizes and Binds to the Promoter of the *Cox-2* Gene (*Ptgs2/PTGS2* Gene)

We investigated the molecular mechanism of MUC1-induced *Cox-2* gene expression in PDA cells. The 5 untranslated region (UTR) of human *Cox-2* gene (*PTGS2/Ptgs2* gene) contains a TATA box and several potential transcriptional regulatory elements such as CRE (cAMP response element) (59/53), NF-IL6 (−132/−124), and NF-κB (−233/−214 and −448/−439), whereas mouse *Cox-2* gene contains CRE-2 (−438/−428), NF-κB (−400/−392), C/EBP (−136/−128), and AP-1 (−67/−62) sites, which are essential for transcriptional regulation of *Cox-2* gene expression. In colon cancer, NF-κB p65 is an important transcriptional regulator of *Cox-2* gene as indicated by attenuation of Cox-2 expression upon NF-κB p65 down-regulation in colon cancer cells.[19,20] To determine if NF-κB p65 is also important for up-regulation of *Cox-2* gene in PDA, we determined Cox-2 levels following the transient knockdown of NF-κB p65 in KCKO and KCM cells. Upon down-regulation of NF-κB p65 subunit, we observed significant attenuation of Cox-2 expression in KCM cells (Fig. 3A, Supplemental Table 3, http://links.lww.com/MPA/A376). In contrast, the level of Cox-2 was unaffected in KCKO cells suggesting that MUC1 cooperates with NF-kbp65 to drive the overexpression of *Cox-2* gene in PDA cells.

To further assess MUC1's role in driving Cox-2 gene expression, we performed Chip assay to test if MUC1-CT and NF-κB p65 bind to the promoter region of *Cox-2* gene (*PTGS2/Ptgs2* gene). Primers were designed to amplify the precipitated chromatin flanking −377/−175 base pairs (bp) upstream (ChIP region I) and +8320/+8550-bp downstream (ChIP region II) of transcription start site of mouse *Cox-2* (*Ptgs2*) gene (Fig. 3B, top panel). Corresponding human-specific primers were designed spanning −346/−118 bp upstream (ChIP region I) and −4053/3820 bp upstream (ChIP region II) of human *Cox-2* (*PTGS2*) gene (Fig. 3B, bottom panel). In Panc02.MUC1, KCM, and HPAFII cells, we observed MUC1-CT and NF-κB p65 binding to the mouse *Cox-2* (*Ptgs2*) or human *Cox-2* (*PTGS2*) promoter ChIP region I, respectively (Fig. 3C, left panel, Supplemental Table 4, http://links.lww.com/MPA/A376). This region contains the NF-κB p65 response element (NF-κB p65 RE). In contrast, Panc02.Neo and KCKO cells did not show strong binding of NF-κB p65 to the same region (Fig. 3C, left panel, Supplemental Table 4, http://links.lww.com/MPA/A376). No significant interaction was observed between MUC1-CT and NF-κB p65 with *Cox-2* (*PTGS2/Ptgs2*) promoter in the control region (ChIP region II) (Fig. 3C, right panels, Supplemental Table 4, http://links.lww.com/MPA/A376) validating the specificity of binding.

To confirm that MUC1 and NF-κB p65 translocate to the nucleus, we assessed the nuclear localization of MUC1 and NF-κB p65 in PDA cell lines. Western blot on the nuclear fraction demonstrated the presence of MUC1-CT in the nucleus of Panc02.MUC1, KCM, HPAFII, and HPAC cells and absence in Panc02.Neo and KCKO cells (Fig. 3D, Supplemental Table 5, http://links.lww.com/MPA/A376). However, we did not observe any significant difference in the nuclear accumulation of NF-κB p65 in the MUC1-null/low (KCKO and Panc02 Neo) versus MUC1-high (KCM and Pan02.MUC1) cells (Fig. 3D), indicating that the nuclear localization of NF-κB p65 is not affected by the absence of MUC1 in these PDA cells. Confocal microscopy further confirmed the colocalization of MUC1 and NF-κB p65 in the cytoplasm and in the nucleus of the KCM cells (Fig. 3E). Taken together, these data suggest that MUC1 binds to NF-κB p65 subunit, translocates to the nucleus, and drives the transcription of *Cox-2* (*Ptgs2/PTGS2*) gene.

Blocking Cox-2 Activity With a Specific Inhibitor, Celecoxib, Reduces Proliferation and Invasion in PDA Cells

We and others have demonstrated that overexpression of MUC1 increases the proliferative index and invasive potential of the PDA cells.[12,21,22] Thus, we questioned if the aggressive phenotype of MUC1-positive PDA cells may be a manifestation of Cox-2 up-regulation in these cells. To test our hypothesis, we blocked Cox-2 activity with celecoxib and analyzed growth and invasive potential of the PDA cells.

A dose-dependent increase in percentage of cells undergoing growth arrest was observed in HPAFII and HPAC cells treated with 50, 75, and 100 μM of celecoxib with18.9%, 42.7%, and 56.4% for HPAFII (Fig. 4A, left panel) and 16%, 47.1%, and 59.6% for HPAC (Fig. 4A, middle panel). In KCKO and KCM cells, a similar dose-dependent increase in percentage of cells undergoing growth arrest was observed upon treatment with increasing dose of celecoxib (Fig. 4A, right panel); however, KCM cells were more resistant to the treatment than KCKO cells. Treatment with celecoxib caused a gradual decrease in the Cox-2 protein expression in all cell lines (Fig. 4B). However, there was no significant change in MUC1 expression upon Cox-2 inhibition (Fig. 4B). The data thus indicated that *Cox-2* is under the regulation of MUC1, but MUC1 is not under Cox-2 regulation. Interestingly, in HPAC cells, we observed a moderate increase in MUC1 expression upon exposure to celecoxib (Fig. 4B, middle panel). Although down-regulation of Cox-2 expression upon celecoxib treatment was comparable in KCM and KCKO cell lines, KCM

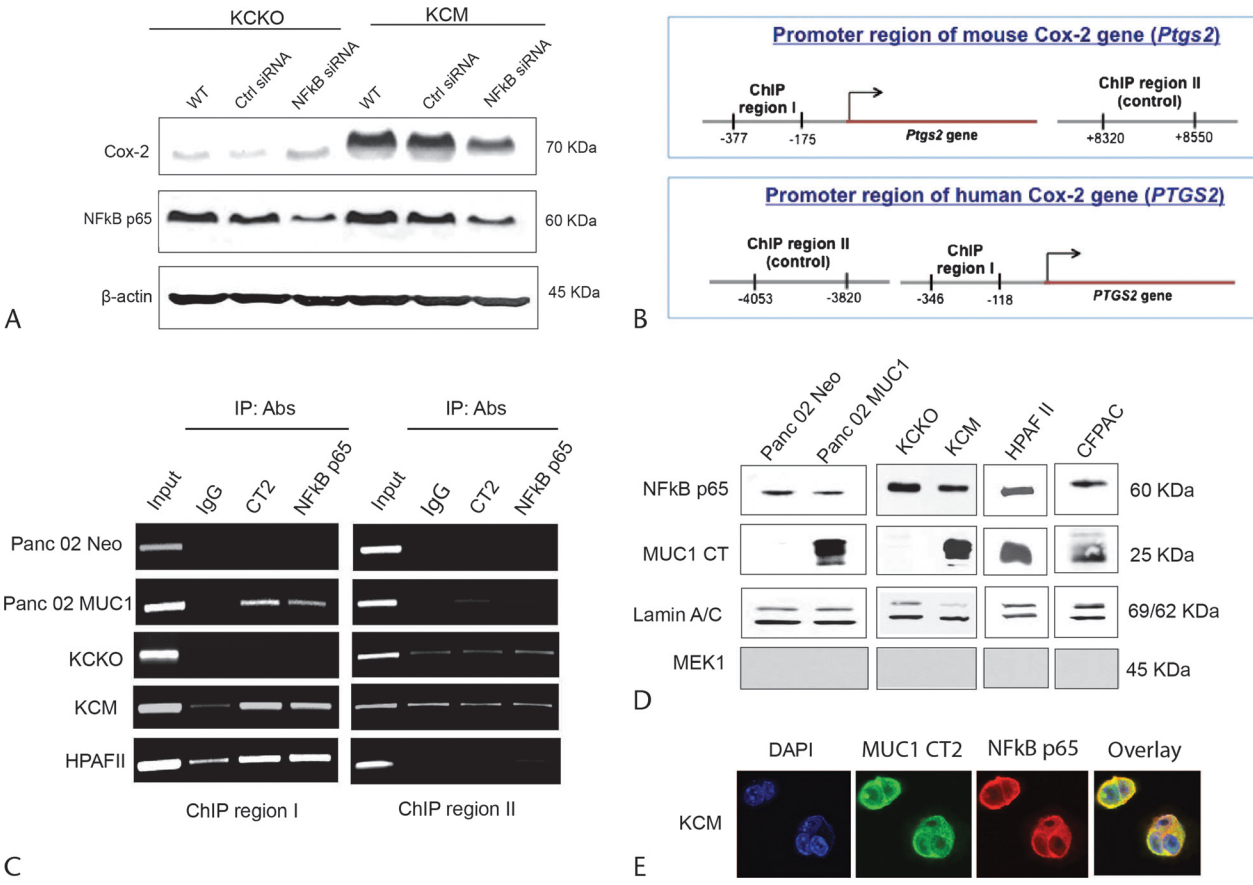

FIGURE 3. Mucin 1 and NF-κB p65 drive the expression of *Cox-2* (*Ptgs2/PTGS2*) gene. A, Nuclear factor κB p65 was transiently knockdown using NF-κB p65–specific siRNA; 72 hours later, Cox-2 and NF-κB p65 levels were analyzed by Western blot; 35 μg of protein was loaded for SDS-PAGE. B, Schematic representation of the promoter region with its putative DNA-binding elements in mouse and human *Cox-2* (*Ptgs2/PTGS2*) gene. C, Sheared chromatin was immunoprecipitated using anti–MUC1-CT antibody CT2 and anti–NF-κB p65 antibody. The immunoprecipitated chromatin was PCR amplified. D, Nuclear lysates were immunoblotted to determine the constitutive nuclear localization of NF-κB p65, MUC1-CT. Lamin A/C was used as a loading control. MEK1 was used as control for cytoplasmic contaminants. E, KCM cells grown on chamber slides were fixed and double stained with anti–NF-κB p65 antibody (red) and anti-MUC1 antibody CT2 (green). Nuclei were stained and mounted with DAPI (blue). Yellow represents overlay of green and red fluorescence suggesting colocalization.

cells were more resistant to growth arrest in comparison to KCKO. This could be due to hyperactivation of the prosurvival pathway such as PI3K/Akt in KCM cells, which counteracts the growth inhibitory effect of celecoxib.[13] The exact mechanisms for celecoxib's anticancer activities are still not clear, but they most likely involve both COX-2–dependent and COX-2–independent mechanisms, as growth arrest was observed regardless of Cox-2 levels in the PDA cells.

We next evaluated the invasive potential of PDA cells upon blocking Cox-2 activity. A 2-fold decrease in the invasive potential of CFPAC cells was observed upon treatment with 15 and 30 μM of celecoxib (Fig. 4C), indicating that Cox-2 is important for the enhanced invasive potential of the MUC1-high PDA cells. Similarly, 1.6-fold (51.6%) and 4.3-fold (19.49%) decrease in the invasive potential of the KCM cells was observed upon treatment of the cells with 15 and 30 μM of celecoxib, respectively (Fig. 4D).

DISCUSSION

The data demonstrate that in PDA cells the proinflammatory-inducible enzyme, Cox-2, is under the regulation of tMUC1. The 2 proteins are abundantly coexpressed in the human and mouse PDA tissues, and their expression increases with stage of the tumor (Fig. 1). Furthermore, overexpression of full-length *MUC1* in PDA cells increases Cox-2 mRNA and protein expression, and conversely, knockdown of MUC1 attenuated Cox-2 mRNA and protein expression (Fig. 2). In most human cell lines tested, high MUC1 levels correlated with high Cox-2 levels except in BxPC3 cells. These cells displayed significantly high level of Cox-2 despite low levels of MUC1 (Fig. 2A). This difference may be due to the presence of normal Kras protooncogene in the BxPC3 cells.[18] All other cell lines tested exhibit mutated Kras. Interestingly, there was no significant difference in the Cox-2 mRNA levels between BxPC3.MUC1 and BxPC3.Neo cells, indicating a possible role of posttranscriptional regulation of *Cox-2* gene by MUC1 in BxPC3 cells (Supplemental Figure 1, http://links.lww.com/MPA/A375 and Supplemental Table 1, http://links.lww.com/MPA/A376). The 3 UTR of Cox-2 mRNA contains the ARE elements that may regulate the stability of Cox-2 mRNA at a posttranscriptional level in BxPC3 cells. The Erk1/2, p38 MAPK, and PI3K pathways have been reported to be instrumental in mediating posttranscriptional regulation of Cox-2 gene.[23] Most of these core signaling pathways are overactivated in cancer cells that overexpress MUC1.[13,16,24]

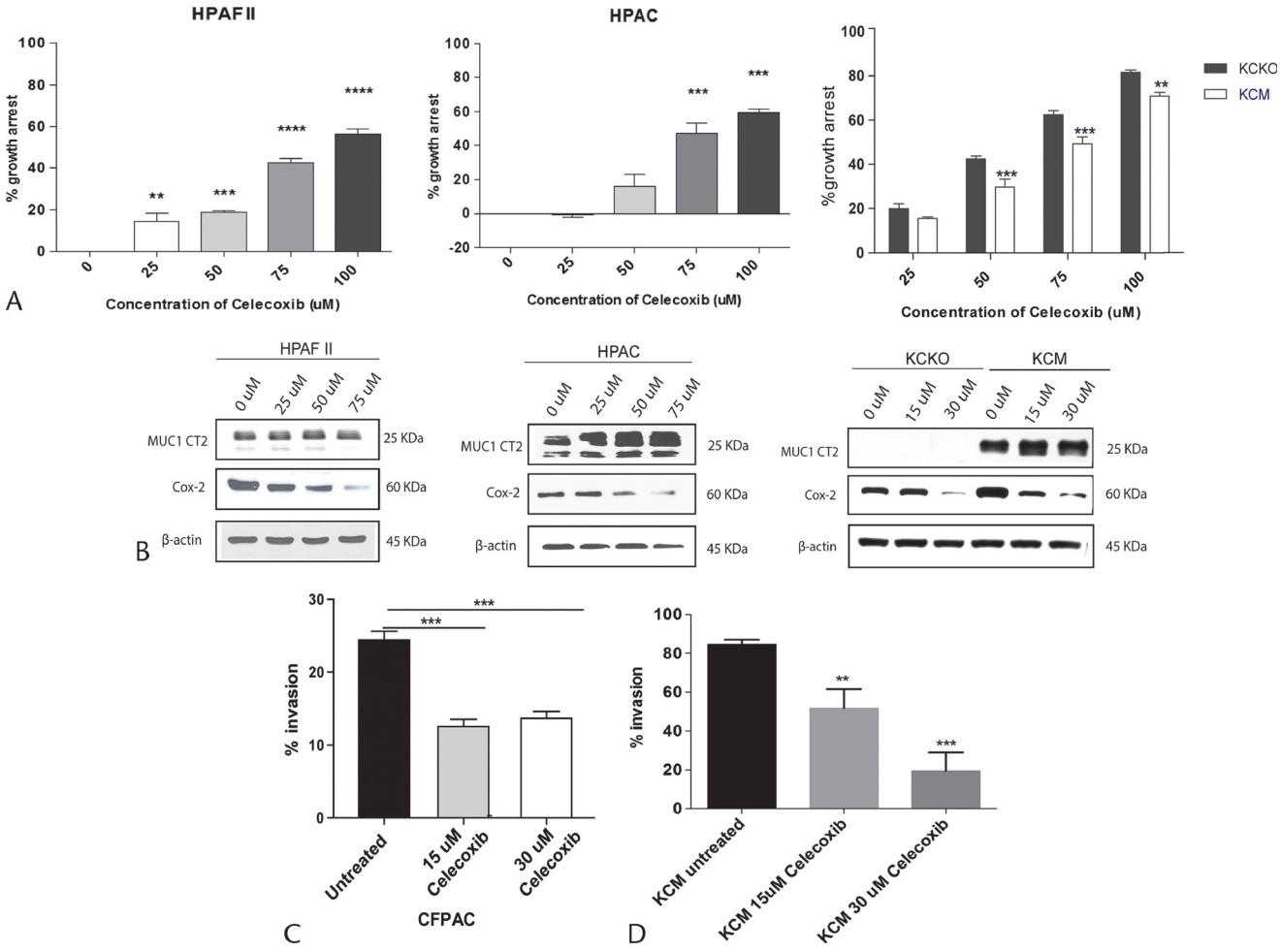

FIGURE 4. Selective inhibition of Cox-2 with celecoxib attenuates the growth and invasive potential of PDA cells. A, MTT assay was performed to determine the growth inhibition following celecoxib treatment. Significant growth arrest is noted in all cell lines tested in response to celecoxib. To determine the statistical significance between celecoxib-treated HPAFII and HPAC cells, 1-way ANOVA was performed, n = 6 (**$P < 0.001$, ***$P < 0.0001$). To determine the statistical significance between celecoxib-treated KCKO and KCM cells, 2-way ANOVA (right panel) was performed, n = 5 (***$P < 0.001$, **$P < 0.01$). B, Cells grown overnight in a 6 well plate were left untreated or treated with indicated concentration of celecoxib for 24 hours. Cell lysates were prepared and were subjected to immunoblotting. The membrane was probed for MUC1 (CT2), Cox-2, and β-actin. No change in MUC1 levels was observed following treatment with celecoxib. C and D, Significant reduction in invasive potential was observed in CFPAC and KCM cells after treatment with celecoxib. One-way ANOVA was performed to determine the statistical significance between celecoxib-treated CFPAC (n = 3, $P = 0.0004$) and celecoxib-treated KCM cells (n = 3, $P = 0.0002$). Percentage of invasion was calculated as absorbance of samples / absorbance of controls × 100.

Thus, a possibility of MUC1 increasing Cox-2 expression posttranscriptionally in PDA cells cannot be overruled. Recently, it was reported that down-regulation of miR-143 in PDA cells increases the stability of Cox-2 mRNA, leading to increased Cox-2 protein in PDA cells.[25] Mucin 1 has been shown to mediate posttranscriptional regulation of 1 of its target gene galectin 3 expression via miR-322.[26]

To elucidate the mechanism by which MUC1 regulates Cox-2 expression, we assessed the (*a*) nuclear accumulation of MUC1 and NF-κB p65 in MUC1-high and -low PDA cells and (*b*) occupancy of MUC1 and NF-κB p65 on the promoter of *Cox-2* (*PTGS2/Ptgs2*) gene by ChIP assay. There was no difference in the nuclear accumulation of NF-κB p65 in MUC1-high and -low PDA cell lines, indicating that the nuclear localization of NF-κB p65 is not affected by the presence or absence of MUC1 in the cells. This observation is in contrast to previous reports that showed decreased nuclear accumulation of NF-κB p65 in ZR-75-1 breast cancer cells upon MUC1 down-regulation.[27] The contrast in observation could arise from differences in tumor origin (breast vs pancreas). Nevertheless, we found that MUC1-CT and NF-κB bind to ChIP region I (within 1000 bp upstream of transcription start site) of the 5′ UTR region of both mouse and human *COX-2/Cox-2* gene. KCKO cells that are null for MUC1 did not show any binding of MUC1-CT and NF-κB p65 to the 5′ UTR of mouse *Ptgs2* gene (Fig. 3). These cells also display low Cox-2 mRNA levels, indicating that the loss of MUC1 attenuates binding of NF-κB p65 to the promoter of *Cox-2* gene and thereby affects the transcription of *Ptgs2* gene. We postulate that during tumor progression, possibly due to hypoglycosylation of MUC1, the MUC1-CT cleaves, associates with NF-κB p65 and translocates as a complex to the nucleus, and binds to the promoter of Cox-2 driving its transcription. The byproduct of Cox-2 enzymatic activity, PGE_2, interacts with its EP receptors and enhances cell survival, proliferation, and invasiveness (Fig. 5).

In colon, breast, PDA, and non–small cell lung cancer (NSCLC), Cox-2/PGE_2 signaling axis promotes proliferation,

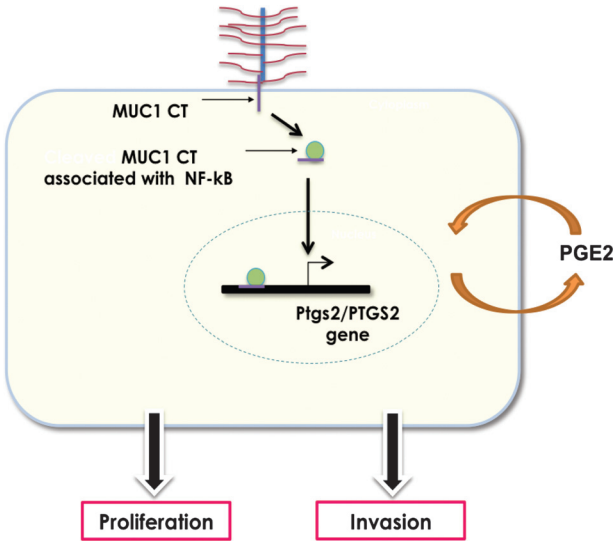

FIGURE 5. Schematic of a model representing the mechanism of Cox-2 regulation in PDA cells. The MUC1-CT undergoes cleavage, associates with NF-κB p65, and translocates as a complex to the nucleus. The transcription complex binds to the promoter of *Cox-2* (*PTGS2/Ptgs2*) gene driving its expression. The byproduct of Cox-2 enzymatic activity, PGE_2, promotes cell survival, proliferation, and invasiveness of cancer cells via engaging with the EP receptors.

survival, and invasion of cancer cells,[28–30] either through decreased production of CD44, MMP-2, and EP4 receptors[31] or by suppressing E-cadherin expression via transcriptional suppressor ZEB1.[32] Thus, lastly, we determined the biological significance of Cox-2 in the MUC1-high PDA cells by blocking the Cox-2 activity. We observed a dose-dependent decrease in growth of HPAFII, HPAC, KCKO, and KCM cells upon treatment with celecoxib underscoring the importance of Cox-2 in proliferation of PDA cells (Fig. 4). Regardless of the levels of Cox-2 or MUC1, all cells responded to Cox-2 inhibition to some degree. Interestingly, KCKO cells that express low levels of Cox-2 as compared with KCM cells were more susceptible to growth inhibition by celecoxib compared with KCM. This may be due to the fact that celecoxib not only inhibits Cox-2 activity, but also modulates cell survival pathways and other cellular responses. A study showed that the antitumor effect of Cox-2 is not entirely contingent upon its ability to inhibit Cox-2 activity but rather to its ability to initiate ER stress.[33] It could be possible that celecoxib initiates ER stress in cells that is counteracted better in MUC1-positive KCM cells, making them more resistant to celecoxib.

Although Cox-2 is overexpressed in MUC1-high PDA cells, the biological effect of Cox-2 may not be the same in all MUC1-high cell lines. We found Cox-2 to be critical for proliferation of HPAFII, HPAC, KCKO, and KCM cells, but not for their invasive potential (data not shown). In contrast, Cox-2 was important for both invasion and proliferation of CFPAC and KCM cells. This variation in the biological effect of Cox-2 could be attributed to the difference in the expression profile of the EP receptors in these cells lines and the subsequent engagement of 1 or more of the signaling pathways downstream of Cox-2/PGE_2 signaling axis. Nonetheless, the significance of Cox-2 overexpression by the MUC1-high cells cannot be underrated, as Cox-2 affects not only tumor cells but also other cellular components in the tumor microenvironment such as immune responses against tumor by recruiting myeloid-derived suppressor cells in the tumor microenvironment. Moreover, Cox-2 is known to regulate vascular endothelial growth factor expression and promote angiogenesis.[34,35] Previously, others and we reported that MUC1 modulates expression of vascular endothelial growth factor in pancreatic and breast cancer cells.[21,36]

Controlling Cox-2 overexpression in cancers remains a challenging task. Our study indicates that MUC1 may serve as an alternative target for blocking Cox-2 overexpression in PDA cells. GO-203, a small molecule inhibitor designed to block MUC-C dimerization and its nuclear translocation, has been shown to reverse MUC1-mediated proliferation in NSCLC and multiple myeloma cells.[37,38] Thus, it might be worth investigating if GO-203 can similarly prevent MUC1 localization to the nucleus and block MUC1-mediated Cox-2 overexpression in PDA cells.

ACKNOWLEDGMENTS

The authors thank the graduate student Michael Shu-Wu at UNC-Charlotte for taking the confocal photographs.

REFERENCES

1. Greenhough A, Smartt HJ, Moore AE, et al. The COX-2/PGE_2 pathway: key roles in the hallmarks of cancer and adaptation to the tumour microenvironment. *Carcinogenesis*. 2009;30:377–386.
2. Koehne C, Dubois R. COX-2 inhibition and colorectal cancer. *Semin Oncol*. 2004;2:12–21.
3. Yip-Schneider MT, Barnard DS, Billings SD, et al. Cyclooxygenase-2 expression in human pancreatic adenocarcinomas treatment of pancreatic cancer. *Carcinogenesis*. 2000;21:139–146.
4. Basu GD, Liang WS, Stephan DA, et al. A novel role for cyclooxygenase-2 in regulating vascular channel formation by human breast cancer cells. *Breast Cancer Res*. 2006;8:R69.
5. Sinha P, Clements VK, Fulton AM, et al. Prostaglandin E_2 promotes tumor progression by inducing myeloid-derived suppressor cells. *Cancer Res*. 2007;67:4507–4513.
6. Williams CS, Mann M, DuBois RN. The role of cyclooxygenases in inflammation, cancer, and development. *Oncogene*. 1999;18:7908–7916.
7. Williams CS, Watson AJ, Sheng H, et al. Celecoxib prevents tumor growth in vivo without toxicity to normal gut : lack of correlation between in vitro and in vivo models. *Cancer Res*. 2000;60:6045–6051.
8. Arber N, Eagle CJ, Spicak J, et al. Celecoxib for the prevention of colorectal adenomatous polyps. *N Engl J Med*. 2006;355:885–895.
9. El-Rayes BF, Zalupski MM, Shields AF, et al. A phase II study of celecoxib, gemcitabine, and cisplatin in advanced pancreatic cancer. *Invest New Drugs*. 2005;23:583–590.
10. Nath S, Mukherjee P. MUC1: a multifaceted oncoprotein with a key role in cancer progression. *Trends Mol Med*. 2014;20:332–342.
11. Wen Y, Caffrey TC, Wheelock MJ, et al. Nuclear association of the cytoplasmic tail of MUC1 and beta-catenin. *J Biol Chem*. 2003;278:38029–38039.
12. Sahraei M, Roy LD, Curry JM, et al. MUC1 regulates PDGFA expression during pancreatic cancer progression. *Oncogene*. 2012;31:4935–4945.
13. Nath S, Daneshvar K, Roy LD, et al. MUC1 induces drug resistance in pancreatic cancer cells via upregulation of multidrug resistance genes. *Oncogenesis*. 2013;2:e51.
14. Tinder TL, Subramani DB, Basu GD, et al. MUC1 enhances tumor progression and contributes toward immunosuppression in a mouse model of spontaneous pancreatic adenocarcinoma. *J Immunol*. 2008;181:3116–3125.
15. Mukherjee P, Basu GD, Tinder TL, et al. Progression of pancreatic adenocarcinoma is significantly impeded with a combination of vaccine and COX-2 inhibition. *J Immunol*. 2009;182:216–224.

16. Besmer DM, Curry JM, Roy LD, et al. Pancreatic ductal adenocarcinoma mice lacking mucin 1 have a profound defect in tumor growth and metastasis. *Cancer Res*. 2011;71:4432–4442.
17. Curry JM, Thompson KJ, Rao SG, et al. The use of a novel MUC1 antibody to identify cancer stem cells and circulating MUC1 in mice and patients with pancreatic cancer. *J Surg Oncol*. 2013;107:713–722.
18. Ura H, Obara T, Nishino N, et al. Cytotoxicity of simvastatin to pancreatic adenocarcinoma cells containing mutant ras gene. *Jpn J Cancer Res*. 1994; 85:633–638.
19. Plummer S, Holloway K, Manson M, et al. Inhibition of cyclo-oxygenase 2 expression in colon cells by the chemopreventive agent curcumin involves inhibition of NF-kappaB activation via the NIK/IKK signalling complex. *Oncogene*. 1999;18:6013–6020.
20. Charalambous MP, Lightfoot T, Speirs V, et al. Expression of COX-2, NF-kappaB-p65, NF-kappaB-p50 and IKKalpha in malignant and adjacent normal human colorectal tissue. *Br J Cancer*. 2009;101:106–115.
21. Roy LD, Sahraei M, Subramani DB, et al. MUC1 enhances invasiveness of pancreatic cancer cells by inducing epithelial to mesenchymal transition. *Oncogene*. 2011;30:1449–1459.
22. Rajabi H, Alam M, Takahashi H, et al. MUC1-C oncoprotein activates ZEB1/miR-200c regulatory loop and epithelial-mesenchymal transition. *Oncogene*. 2014;33:1680–1689.
23. Dixon D. Dysregulated post-transcriptional control of COX-2 gene expression in cancer. *Curr Pharm Des*. 2004;10:635–646.
24. Hattrup CL, Gendler SJ. MUC1 alters oncogenic events and transcription in human breast cancer cells. *Breast Cancer Res*. 2006;8:R37.
25. Pham H, Rodriguez CE, Donald GW, et al. miR-143 decreases COX-2 mRNA stability and expression in pancreatic cancer cells. *Biochem Biophys Res Commun*. 2013;439:6–11.
26. Ramasamy S, Duraisamy S, Barbashov S, et al. The MUC1 and galectin-3 oncoproteins function in a microRNA-dependent regulatory loop. *Mol Cell*. 2007;27:992–1004.
27. Ahmad R, Raina D, Joshi MD, et al. MUC1-C oncoprotein functions as a direct activator of the nuclear factor-kappaB p65 transcription factor. *Cancer Res*. 2009;69: 7013–7021.
28. Ding XZ, Hennig R, Adrian TE. Lipoxygenase and cyclooxygenase metabolism: new insights in treatment and chemoprevention of pancreatic cancer. *Mol Cancer*. 2003;2:10.
29. Howe LR. Inflammation and breast cancer. *Breast Cancer Res*. 2007;9:210.
30. Zhu M, Zhu Y, Lance P. TNFα-activated stromal COX-2 signalling promotes proliferative and invasive potential of colon cancer epithelial cells. *Cell Prolif*. 2013;46:374–381.
31. Dohadwala M, Batra RK, Luo J, et al. Autocrine/paracrine prostaglandin E_2 production by NSCLC cells regulates matrix metalloproteinase-2 and CD44 in cyclooxygenase-2–dependent invasion. *J Biol Chem*. 2002; 277:50828–50833.
32. Dohadwala M, Yang SC, Luo J, et al. Cyclooxygenase-2–dependent regulation of E-cadherin: prostaglandin E(2) induces transcriptional repressors ZEB1 and snail in non–small cell lung cancer. *Cancer Res*. 2006;66:5338–5345.
33. Chuang HC, Kardosh A, Gaffney KJ, et al. COX-2 inhibition is neither necessary nor sufficient for celecoxib to suppress tumor cell proliferation and focus formation in vitro. *Mol Cancer*. 2008;7:38.
34. Yoshida S, Amano H, Hayashi I, et al. COX-2/VEGF-dependent facilitation of tumor-associated angiogenesis and tumor growth in vivo. *Lab Invest*. 2003;83:1385–1394.
35. Liu H, Yang Y, Xiao J, et al. COX-2–mediated regulation of VEGF-C in association with lymphangiogenesis and lymph node metastasis in lung cancer. *Anat Rec*. 2010;293:1838–1846.
36. Woo JK, Choi Y, Oh SH, et al. Mucin 1 enhances the tumor angiogenic response by activation of the AKT signaling pathway. *Oncogene*. 2012;31: 2187–2198.
37. Raina D, Kosugi M, Ahmad R. Dependence on the MUC1-C oncoprotein in non–small cell lung cancer cells. *Mol Cancer Ther*. 2011;10:806–816.
38. Yin L, Ahmad R, Kosugi M, et al. Survival of human multiple myeloma cells is dependent on MUC1 C-terminal transmembrane subunit oncoprotein function. *Mol Pharmacol*;2010:166–174.